Fast proton-induced electron emission from rare-gas solids and electrostatic charging effects

R. A. Baragiola, M. Shi, R. A. Vidal, and C. A. Dukes
Laboratory for Atomic and Surface Physics, Engineering Physics, University of Virginia, Charlottesville, Virginia 22901
(Received 3 April 1998)

We have studied electron emission from solid Ar, Kr, and Xe films induced by impact of 10–100 keV protons at normal incidence. Electron yields were measured as a function of applied anode voltage and film thickness from 200 to 7000 Å. The observed electron yields are huge—hundreds of electrons per incident ion: higher, per amount of electronic energy deposited, than for any other material studied so far. We extend an electron emission model, developed for metals, to the case of insulators, and obtain electron escape depths of hundreds of nm when fitted to the dependence of electron yield on target thickness. The experiments, especially those with Ar and Kr, are not well described by the model. The reason is the presence of strong electric fields produced by charged traps in the films which, together with a low surface barrier (absence in the case of Ar) ease the extraction of electrons from the films at sufficiently high anode voltages. A hysteresis in the electron currents as a function of anode voltage is also attributed to macroscopic charging of the films. The electrostatic surface potential of the films during ion bombardment is derived by comparing the dependence of the electron emission current with anode voltage to results of computer simulations of electron trajectories near the sample. [S0163-1829(98)07940-5]

I. INTRODUCTION

Electron emission from insulators under light ion bombardment has been investigated far less than for metals due mainly to problems of sample preparation and electric charging during bombardment. The electron emission yield (number of electrons emitted per incident particle) induced by energetic *electrons or photons* is up to about an order of magnitude larger for insulators than for other materials;[1–3] this has favored the use of oxide surfaces for electron multipliers. Large electron yields have been attributed to larger electron escape depths and lower surface barriers in insulators. The effect of the band gap E_g of insulators and semiconductors on electron emission has been discussed by Grais and Bastawros[4] using a model[5] to analyze electron impact experiments. They found that for semiconductors the electron yields do not vary with E_g, while for insulators the yields first increase with E_g, pass through a maximum at $E_g \sim 7$ eV, and then decrease with E_g. This dependence can be understood to result from competing processes: a large band gap gives a low probability for energy loss by secondary electrons and hence large escape depths but requires more projectile energy transfer to excite the electrons.

Electron emission from some insulators bombarded with protons and other ions has been measured as well.[6–11] In general, the phenomenon shows similar characteristics as photoelectron or secondary electron emission.[12] However, fast ions can produce a high density of ionizations in the solid along their penetration path (track).[13] Different studies on ion-bombarded polymers,[14] silicon oxide,[9] and water ice[11] have shown that unbalanced holes in the ionization track during electron emission can produce an electrical potential that acts to oppose electrons leaving the solid. This can be viewed as the effect of a local charging of the material in each individual ion track. An additional, macroscopic, charging that also acts to hinder electron emission results from the cumulative effect of many projectiles producing relatively long-lived and localized (trapped) charges. Effects of charging on electron emission from rare-gas solids have been seen under x-ray[15] and VUV irradiation.[16,17]

Current theories of ion-induced electron emission have been covered in several review articles;[12–23] they do not include ionization track effects and rarely address in any detail other issues particular to insulators.[22] The scarcity of experimental data and the complexity of the physical processes involved have prevented the development of a comprehensive theoretical picture. This prompted our current studies aimed at identifying the main physical mechanisms acting on electron emission. Here we have chosen the rare-gas solids Ar, Kr, and Xe as target materials because they present several advantages. Their electronic states are well known and their band gap is high, so thermal effects can be neglected. Since they are inert, chemical alteration during bombardment is ruled out. Also, the fact that they are weakly bound allows their description as condensed gases and the application of extant knowledge of gas-phase collision processes. Electron emission from films of rare-gas solids has been studied by Gullikson and Henke for the case of dilute ionizations produced by high-energy x rays[15,24] and positrons,[25] and analyzed without consideration of the presence of holes or the image potentials they create near an interface.

Below we present measurements of electron yields from thin films of Ar, Kr, and Xe under bombardment by protons at normal incidence, as a function of projectile energy in the range 10–100 keV, applied anode voltage, and film thickness. We then discuss a model for electron emission, electron escape, and surface charging.

II. EXPERIMENTS

The apparatus for measuring electron emission has been described by Shi *et al.*[11] The experiments were made in an ultrahigh vacuum chamber (base pressure in the 10^{-10} Torr range) connected to the University of Virginia 120 kV heavy

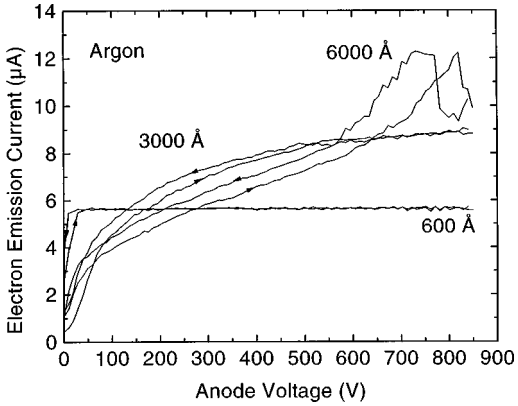

FIG. 1. I-V_a characteristic for electron emission from Ar films of different thickness under bombardment with 55-keV protons at normal incidence. The arrows indicate the direction in which the anode voltage is scanned. The proton current is 18 nA.

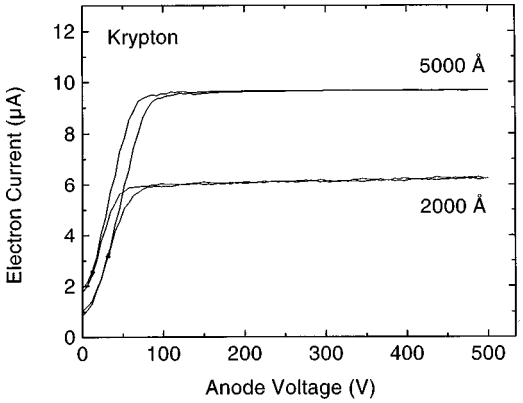

FIG. 2. Same as Fig. 1 but for Kr films. The proton current is 22 nA for the 2000-Å Kr film and 14 nA for the 5000-Å Kr film.

ion accelerator. Research grade gases (purity>99.997%) were condensed onto the gold electrode of a quartz crystal microbalance,[26] cooled by a closed-cycle refrigerator. The polycrystalline gold substrate was cleaned by sputtering with 5 keV Ar ions; the cleanliness was verified by measuring the electron yield using protons and comparing with previous results.[1] A clean substrate is important since it has been observed that insulating layers (e.g., an interface oxide) can decrease the electron emission yields from rare gas films,[27] possibly because hole neutralization is hindered at the substrate. The films, which are expected to be polycrystalline,[28] were grown right after cleaning the substrate; growth temperatures were 20 K for Ar and 24 K for Kr and Xe. The ion beam, collimated by a 5-mm-diam aperture, was incident normal to the surface of the films; ion current densities were between 40 and 300 nA/cm^2. Irradiation fluences were kept below 10^{15} ions/cm^2 low to avoid significant changes in film thickness due to sputtering and trapping of scattered protons in the films.

A cylindrical aluminum anode that also acts as a heat shield surrounds the sample. The electron emission current was obtained from the change in the target current when the anode was biased positively. The electron yields are then simply the ratio of the electron to ion currents.

III. RESULTS

A. I-V characteristics

For the three rare-gas solids, the electron yields are huge, more than two orders of magnitude larger than what can be obtained from clean metal samples. Figure 1 shows the I-V_a characteristics (electron emission current I versus applied anode voltage V_a) for the case of Ar films bombarded by 55-keV protons. The measurements were made by scanning V_a up and down at a rate of 38 V/s and are consistent with previous measurements.[8] With increasing V_a the electron emission current reaches a saturation value, but only for thin films as observed previously using photon excitation.[16,17,29,30] In contrast with the I-V_a characteristics of the bare gold substrate, which saturates at a few volts, the I-V_a curves for the condensed films saturate at relatively high voltages, for instance, approximately 50 V for a 600-Å argon film. The need for a higher saturation voltage indicates that the films charge up to a positive potential during electron emission. For a 3000-Å Ar film, the electron emission current grows slower with V_a; saturation is achieved at a few hundred volts, indicating a larger positive film potential. For a 6000-Å film, the electron emission current increases fast below 50 V and then grows steadily without showing any saturation. Higher anode voltages produce dielectric breakdown in the film, as previously reported.[8]

In the case of Kr and Xe, we always observed a saturation behavior of the I-V_a curves up to the largest thickness tried, ~7 000 Å. We have not observed breakdown for these targets. Figures 2 and 3 show I-V_a curves for 55-keV protons incident on Kr and Xe films of different thicknesses. The electron emission currents begin to saturate when V_a is between 40 and 80 V. The voltage at the knee of the I-V_a curve increases with film thickness and is larger for Kr than for Xe. For these films, a slight slope of the I-V_a curves is observed at large V_a. For all the condensed films we find that the electron emission currents are substantial for $V_a=0$ and that the I-V_a curves have hysteresis; the curve measured with increasing V_a lies below that obtained with decreasing V_a. This effect is reversible since the I-V curves are reproduced over several cycles. The origin of the hysteresis effect, also reported previously for Ar films,[8,31] is attributed to macroscopic charging and will be discussed below. The area of the hysteresis loop increases with the speed at which V_a is scanned and decreases with increasing ion beam current.

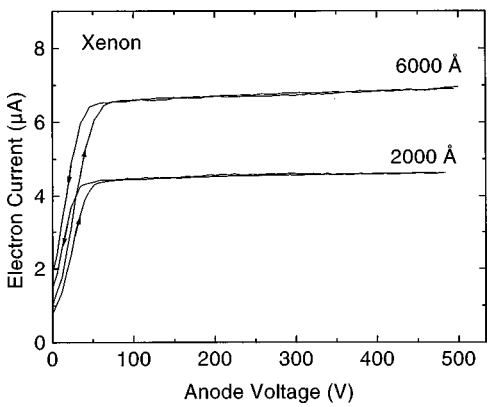

FIG. 3. Same as Fig. 1 but for Xe films. The proton current is 18 nA.

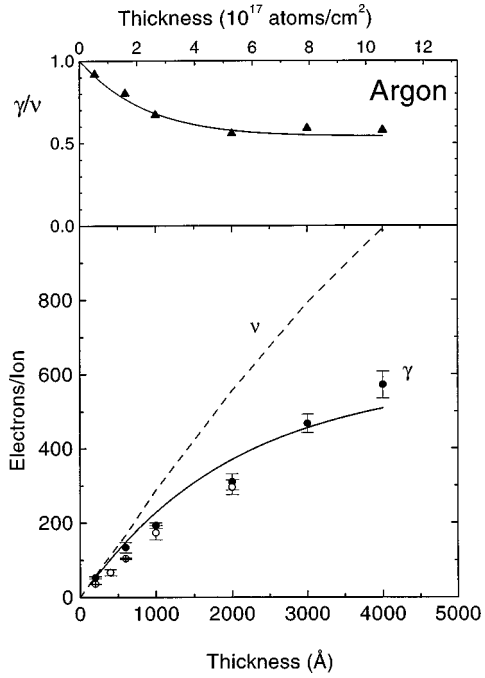

FIG. 4. Electron yields and ratio of electron yields to the number of electron-hole pairs in the film vs film thickness for the bombardment of Ar films at 20 K with 33-keV protons at normal incidence. The solid line in the lower panel is a fit to Eq. (2) (see text); ●, electron yield for fast film grow rate and—fit; ○, electron yield for slow film grow rate. The dashed line is the calculated number of electron-hole pairs. The line in the upper panel is to guide the eyes and has no other meaning.

An interesting observation in the case of Ar, but not Kr or Xe, films is that the electron yields were ~20% lower for films grown at a low rate, ~1.5 Å/s, compared to typical rates of ⩾10 Å/s. The lower yields are attributed to an enhanced formation of voids[32,33] in the Ar films during slower growth; these voids can act as electron traps due to the negative electron affinity of solid Ar.[34] Since it is possible that electrons may be trapped in defects such as vacancies created by the ion beam we searched for a possible effect of irradiation fluence (exposure) on the yields. We saw no fluence dependence for fluences up to 2.5×10^{15} ions/cm^2, in contrast with the complex behavior seen for x-ray irradiation of Xe by Gullikson and Henke,[15] which may be related to contamination from background gases in their moderate vacuum (10^{-7} Torr).

B. Film thickness dependence of electron yields

In Figs. 4–6 we present the electron yields for 33-keV proton impact, obtained from the saturation values of the anode currents, as a function of the film thickness. The contribution of electron emission from the substrate to the total emission current can be neglected except for very small thicknesses since the electron yields for protons on gold[1] are smaller than 2.5. As mentioned above, for Ar films thicker than 4000 Å it was not possible to achieve saturation in the electron emission current even using the maximum anode voltage (1000 V) allowed by our experimental setup.

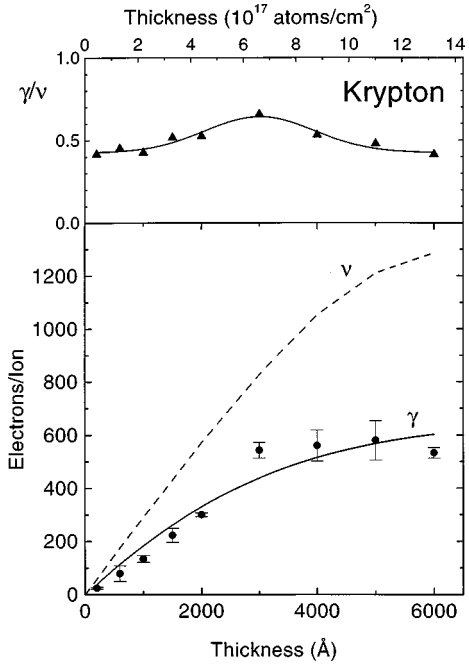

FIG. 5. Same as Fig. 4 but for Kr films at 24 K.

IV. DISCUSSION

To analyze the results we start with the standard electron emission theory[1] generalized to include insulators. A light ion penetrating an insulator film loses energy mainly by electronic excitations and by generating electron-hole pairs along its track. These pairs are produced very fast, in times of the order of 10^{-16}–10^{-14} s after the passage of the projectile, as a result of ionizations produced directly by the ions, Auger decay of inner-shell vacancies, and ionizations created by

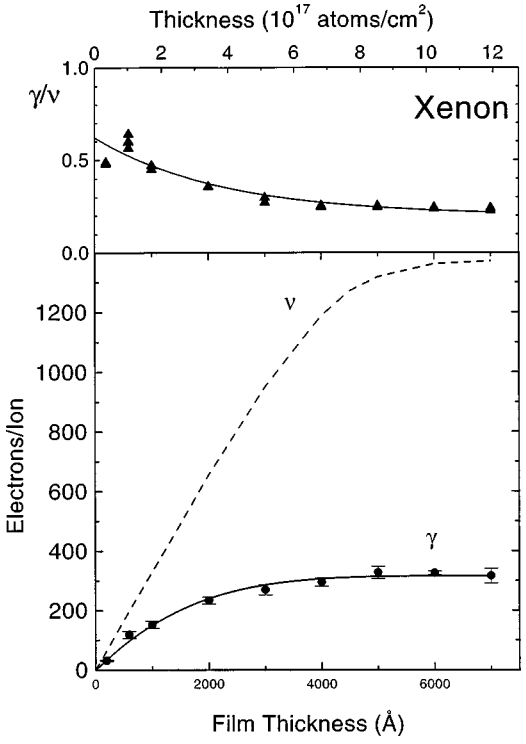

FIG. 6. Same as Fig. 4 but for Xe films at 24 K.

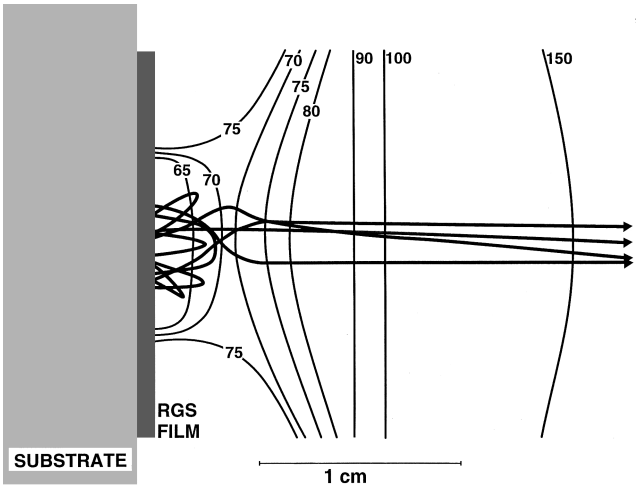

FIG. 7. Contours of electrostatic potential in volts and some representative trajectories of electrons emitted from the film at random points of ion impact, angles of emission, and electron energies in the range 5–10 eV. For the simulation, the beam spot is at 80 V, the substrate at 0 V, and the anode at 320 V. The ion beam comes from the right. The thickness of the film is exaggerated for clarity.

fast secondary electrons in a cascade of collisions.[35] A small fraction of electrons will be ejected into vacuum or injected into the substrate before this ionization cascade is over. After the kinetic energy of the electrons falls below E_g further ionization is not possible. The total number of electron-hole pairs produced, ν, can be estimated by integrating $D_e(z)$, the electronic deposited energy per unit depth z over the thickness of the film, d:

$$\nu = \int_0^d \frac{D_e(z)}{w}\, dz, \tag{1}$$

where w is the differential energy required for the production of a free electron-hole pair in the solid.[36] After ionization is complete, electrons and holes will drift inside the film subject to scattering by the lattice atoms, and electric fields due to the ionization track, image charges induced in the substrate, and the externally applied anode potential. Electrons will lose energy as a result of excitations until their kinetic energy falls below the excitonic band gap, and then very slowly as a result of phonon excitation. If the electrons reach the surface with energy above the vacuum level, they may be emitted into vacuum. The number of electrons arriving at the surface with energies exceeding the vacuum level will be attenuated as some of them fall below this energy due to collisions. Excited electrons eventually slow down to thermal energies and recombine with holes, become trapped at defects inside the film or go to the substrate. If the solid has negative electron affinity, such as Ar, even thermalized electrons can escape the solid into vacuum if their accompanying holes are neutralized at the substrate.

A. Case of weak internal electric fields: exponential electron attenuation

So far, the effect of electron attenuation on electron emission from insulators has been considered in the case of dilute ionizations caused by low fluences of x rays or electrons. In such cases where electrostatic forces due to holes can be neglected, an exponential law $e^{-z/L}$ can model the fraction of electrons surviving attenuation, where L is called the electron escape depth. In this approximation, the electron yield γ is given by[1]

$$\gamma = Pf \int_0^d \frac{D_e(z)}{w}\, e^{-z/L} dz, \tag{2}$$

where f is the fraction of the electrons that travel towards the surface, and P is the probability that an electron that reaches the surface is transmitted into vacuum. For isotropic electron cascades in a planar geometry, $f=0.5$, but since the primary ionizations eject electrons predominantly in the forward direction, $f<0.5$.[37–40] The quantities P and L should be interpreted as averages over the electron energy distribution.

In the case of metals or semiconductors, L is very small, 5–15 Å,[23] due to strong inelastic scattering with valence electrons. Over this short distance, we can approximate $D_e(z) \approx S_0 = dE(E_0)/dx$, the electronic stopping power taken at the incident energy E_0, where x is the distance along the path of the ion. Figures 4–6 already suggest that the electron escape depths are of the order of thousands of Å for the rare gas solids. Since protons in our energy range slow down significantly over those distances we do not assume that $D_e(z)$ is constant but rather evaluate it accurately using the TRIM Monte Carlo simulation code.[41] This program takes into account projectile slowing down and scattering during penetration and the effect of projectile reflection from the substrate. For the simulations, TRIM uses a fit of S_0 to experimental data on gas targets assuming that S_0 is proportional to $E^{1/2}$ in the limit of low energies. In the absence of data for solids, the use of S_0 for gases is justified since the energy levels are only slightly modified for the rare gases used in this work. The values obtained by TRIM for $D_e(z)$ are adjusted so that $D_e(0)$ equals the value of S_0 measured in low-energy experiments.[42] Based on experiments and simulations on gases[36] and solid Ar,[43] we take $w \approx W$, the average energy for the production of an electron-hole pair. This approximation should be good for proton energies down to about 1 keV; at lower values, energy loss due to elastic collisions with target atoms becomes a sizable fraction (>10%) of the inelastic energy loss. We use the compiled values of W (Ref. 44) listed in Table I.

TABLE I. Electron affinity U (Ref. 44), mean energy to produce an electron-hole pair (Ref. 44), W, electron escape depths L and fraction of emitted electrons Pf for rare-gas solids bombarded by 33-keV protons. Only in the case of Xe is the attenuation represented closely by an exponential function with a decay constant L.

Target	U (eV)	W (eV)	L (μm)	Pf
Ar	−0.3	27±1	0.24±0.02	1.0
Kr	0.3	25±1	0.19±0.04	0.83
Xe	0.4	24±1	0.18±0.02	0.70

In Figs. 4–6 we show the ratio between experimental electron yields γ and electron-hole pairs ν, calculated with Eq. (1). We fit our experimental electron yields with Eq. (2) to obtain values for the electron escape depth L and the product Pf, which are shown in Table I together with values of

the surface barrier U (electron affinity). The values of L, around 0.2 μm, can be compared with $L=0.1-0.4$ μm reported for the transmission of $\lesssim 3$ eV electrons through films of rare gas solids,[44] and the values of 0.45 μm for Ar and 0.23 μm for Xe obtained by modeling x-ray photoelectron emission experiments.[45] Since Ar has a negative electron affinity, a finite attenuation length cannot result from electron energy loss; i.e., even electrons at the bottom of the conduction band can leave the solid. Therefore, attenuation has to be due to recombination with holes or trapping. Possible traps are vacancy clusters or voids that trap electrons because of the negative electron affinity, or impurities that capture electrons to form negative ions.

Although the values of the attenuation lengths are of the order of those reported for experiments using low fluences of weakly ionizing electrons or x rays,[15] the fits cannot be considered satisfactory. This is because the fitted values of Pf are larger than 0.5, the value to which they are bound in the model ($P\leqslant 1$ and $f\leqslant 0.5$). Values of $f>0.5$ have been noticed by Schwentner in photoemission experiments;[17] he concluded that they are due to the additional electron emission produced at the substrate. However, we observe $f>0.5$ for energetic ion impact, where electron emission from the substrate is negligible compared with that from the bulk of the film. We therefore propose that the anisotropy is real: there are more electrons in the film traveling towards the surface than towards the substrate. Such an anisotropy can be produced by an electric field inside the film, like the internal fields larger than 1 kV/cm inferred by Grosjean, Baragiola, and Brown[31] to occur in MeV ion bombardment of thin ($\sim$1000 Å) Ar films with positive anode voltages. We note that fields above 10 kV/cm saturate the drift velocity of electrons in the rare-gas solids[46] and even higher fields[47] are needed to prevent the recombination of electron-hole pairs at the values of S_e pertinent to this work.

B. Case of strong electric fields and electrostatic charging

To estimate the internal fields in the films, we model the I-V_a curves calculating the electrostatic potential and electron trajectories in the region surrounding the target using the three-dimensional finite element program SIMION.[48] In the simulation, electrons of randomly chosen energies in the range 5–10 eV start in vacuum from the ion beam spot at random positions and angles randomly chosen within a cosine distribution with respect to the surface normal. Keeping the substrate and the target block at ground potential, the beam spot voltage V_s is varied for different values of the (positive) anode voltage V_a and the fraction of the electrons reaching the anode is recorded. Not all electrons emitted from the film reach the anode, even if $V_s<V_a$ since a potential barrier can result in front of the film due to the closeness to the grounded substrate (see Fig. 7). This condition is not unique to our setup but is typical of experiments of particle irradiation of insulators.

We obtained a set of surface potentials that would make the fraction of electrons reaching the anode equal to the measured γ_a/γ_s where γ_a is the measured electron yield at a given V_a, averaged between increasing and decreasing V_a and γ_s is the saturation yield at high V_a. Figure 8 shows the thickness dependence of the surface potential of Ar films for

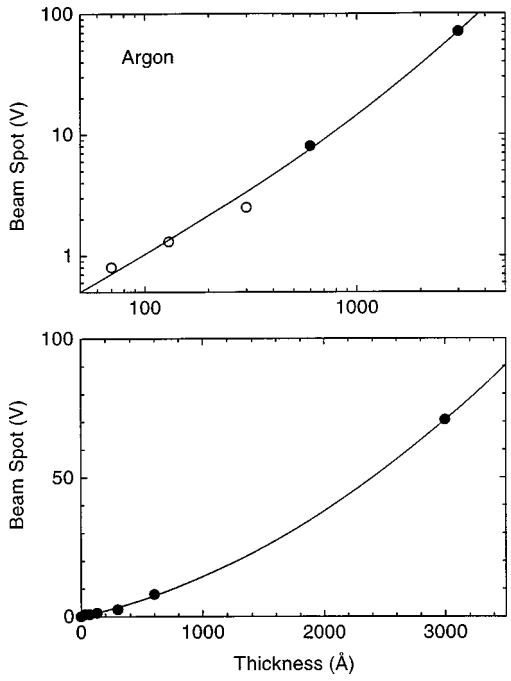

FIG. 8. Potential at the beam spot for an electron emission current 84% of the saturation value, for 33-keV protons on solid Ar as a function of film thickness (●). Also shown are values derived from the photoemission peak shifts measured by Schwentner *et al.* (Ref. 16) during x-ray irradiation of thin Ar films (○). The voltage scale is logarithmic in the top graph and linear in the lower graph.

$\gamma/\gamma_s=0.84$, a condition close to saturation. The surface potential is seen to grow quadratically with film thickness. The results are quite consistent with those found for much thinner films during photon irradiation of thin films[16,17] and calculated from the shifts in photoelectron energies. The surface potentials for 2000–6000 Å Kr and Xe films are 10–15 V and therefore quite sensitive to the assumed initial energy of the emitted electrons.

In the current and previous experiments, the nature of the charge has not been identified; it may be located for instance at ionized impurities or at host ions trapped at defect sites. We can calculate the magnitude of this trapped positive charge from the surface potential in two simple cases: (a) a uniform distribution of charges at the surface with areal density σ in q/cm^2, where q is the elementary charge, and (b) a uniform charge distribution in the volume with density ρ (q/cm^3). Case (a) is that of a plane electrostatic capacitor; the potential inside the film as a function of distance from the substrate z is given by

$$V(z)=\sigma z/(\varepsilon\varepsilon_0), \tag{3}$$

where ε is the static dielectric constant of the rare-gas solid: 1.56, 1.78, and 1.98 for Ar, Kr, and Xe, respectively,[49] and ε_0 is the permittivity of vacuum, 8.854×10^{-14} C V^{-1} cm^{-1}. The surface potential V_s in volts, for a film of thickness d in cm is given by

$$V_s=1.81\times10^{-6}\sigma d/\varepsilon. \tag{4}$$

The amount of surface charge density that can be sustained may be limited to a value, $V_{s,\max}\approx 10^7\ d$, that produces an electric field of $\sim$10 MV/cm where a significant field elec-

tron emission current will be drawn from the metal substrate.[50] Part of the field emitted electron current will recombine with the surface charge self-limiting it. The value of $V_{s,\max}$ implies $\sigma \lesssim 10^{13}\ q/\mathrm{cm}^2$. We note that the potentials V_s determined in this study are always below $V_{s,\max}$.

In case (b), the potential inside the film is given by

$$V(z) = \rho z(d - z/2)/(\varepsilon \varepsilon_0), \tag{5}$$

where ρ is the charge density trapped in the volume. Thus, the surface potential increases quadratically with the thickness of the film:

$$V_s = 0.9 \times 10^{-6} \rho d^2/\varepsilon. \tag{6}$$

In this case the electric field is not constant inside the film but decreases linearly from a maximum value of $E_{\max} = \rho d/(\varepsilon \varepsilon_0)$ at the substrate. The same argument about field emission can be applied here, giving $V_{s,\max} \approx 5 \times 10^6 d$ and $\rho \lesssim 10^{13}/d$. Thus the quadratic growth of the surface potential with d should eventually slow down at large thicknesses, limited by field emission from the substrate.

The surface potential of Ar shown in Fig. 8 can be fitted to the expression $V_s = (1.0 \pm 0.1) \times 10^6 d + (4.6 \pm 0.3) \times 10^{10} d^2$. The two terms correspond to the superposition of effects produced by a surface charge $\sigma = 9 \times 10^{11}\ q/\mathrm{cm}^2$ (linear term) and a bulk charge density $\rho = 8 \times 10^{16}\ q/\mathrm{cm}^3$ (quadratic term). The value of σ corresponds to a concentration of ~ 0.001 holes per surface atom whereas the value of ρ represents a volume concentration of $\sim 3 \times 10^{-6}$ holes per Ar atom. This value may be a result of an impurity content of this magnitude but the consistency of the surface potentials with those derived from the experiments of Schwentner[17] made under different conditions, suggest that intrinsic traps may be responsible for the charging behavior. The intrinsic holes (Ar^+ and Ar_2^+) cannot, however, be responsible for this behavior since, as we show below, their equilibrium concentration is too small. As an upper limit, neglecting recombination, the equilibrium hole concentration is given by $p = J\nu\tau/d = 1/2 J\nu/u$, where J is the beam current density, τ the mean hole lifetime (transit time to the substrate) and u the mean hole velocity in the film. Using the low hole mobility of Ar_2^+, $\mu = 0.02\ \mathrm{cm}^2\ \mathrm{s}^{-1}\ \mathrm{V}^{-1}$,[44] an electric field of 10^6 V/cm, we obtain hole lifetimes τ of the order of ns, and concentrations of only $\sim 10^8/\mathrm{cm}^3$ at the current densities used. This value is nine orders of magnitude lower than that of ρ given above. This points to the need to postulate deep, relatively immobile traps with lifetimes of the order of seconds, the delay time seen in the hysteresis behavior, to explain macroscopic charging.

The fact that the value of the surface charging does not depend on ion beam current over a range of 0.1–10 nA shows that the rate of decay of the traps depends on current as is the case for the ionization rate. This can be understood if the lifetime of a trap during irradiation is mainly limited by the availability of electrons that can neutralize it, rather than by drift to the substrate.

The surface potential will then have two effects. On one hand, it will enhance electron emission by causing a larger fraction of the electrons liberated inside the film to reach the surface and by pushing mobile holes into the substrate. On the other hand, the potential will hinder emission (unless the external field is high enough) by causing a potential barrier in front of the surface. The fact that charging increases the yields at anode voltages insufficient to cause saturation shows that the predominant effect of the resulting electric field is to induce anisotropy in the electron flux inside the film, with more electrons moving towards the surface than towards the substrate. A secondary effect of the internal electric field is to heat up the electrons so that they can more easily surmount the surface barrier. This is a likely explanation for the small slope of the I-V curves at high anode voltages for Kr and Xe, which have a positive surface barrier. We expect that the recombination of electrons and intrinsic holes is not important in these materials because an electron that is slow enough to recombine is also below the vacuum level and not able to escape into vacuum. In the case of Ar, however, where even thermalized electrons may escape due to the negative electron affinity, recombination competes with electron emission.

V. CONCLUSIONS

Ion-induced electron yields from Ar, Kr, and Xe ice films bombarded by keV protons depend on film thickness and are very large (several hundred/proton) for thick films (>4000 Å). This is partly due to long electron escape depths and low surface barriers in rare-gas solids. The I-V_a collection curves show saturation for anode voltages in the films for Kr and Xe films and thin Ar films, but not for thick Ar films. A simple model, a straightforward extension of models originally made for metals, gives electron escape depths of tenths of microns when fit to experiments. However the collection of more than 50% of excited electrons for Kr films and near 100% for thin Ar films, indicate the existence of a large internal electric field that drives the electrons to the surface. We associate this field to the presence of charged traps in the film which lead also to a high surface potential, responsible for the large anode voltages needed to saturate the emission current. Modeling the I-V curves allows deriving the surface potential, which is found to increase with film thickness. This variation is consistent with the existence of surface and bulk densities of traps that do not depend strongly on film thickness.

In the case of thin Ar films, the nearly complete collection at the anode of the electrons freed in the bulk is made possible both by the negative electron affinity of the surface and by the high internal electric field that separates the electron-hole pairs preventing recombination. For thick Ar targets, the electric field leads to dielectric breakdown.

ACKNOWLEDGMENTS

We thank D. E. Grosjean and W. L. Brown for useful discussions. This work was supported by the National Science Foundation, Division of Materials Research and Division of International Programs, and by NASA Magnetospheric Physics Program. R.A.V. has received support from the Consejo Nacional de Investigaciones Científicas y Técnicas of Argentina and from Fundación Antorchas.

[1] R. A. Baragiola, E. V. Alonso, and A. Oliva-Florio, Phys. Rev. B **19**, 121 (1979).
[2] E. V. Alonso, R. A. Baragiola, J. Ferrón, and A. Oliva-Florio, Radiat. Eff. **45**, 119 (1979).
[3] Z. Y. Zhao, A. M. Arrale, S. L. Li, F. D. McDaniel, S. Matteson, D. L. Weathers, J. M. Anthony, and B. Gnade, Nucl. Instrum. Methods Phys. Res. B **99**, 30 (1995).
[4] K. I. Grais and A. M. Bastawros, J. Appl. Phys. **53**, 5239 (1982).
[5] G. F. Dionne, J. Appl. Phys. **44**, 5361 (1973).
[6] E. V. Alonso, R. A. Baragiola, J. Ferrón, and A. Oliva-Florio, Radiat. Eff. **45**, 119 (1979).
[7] J. Ferrón, E. Alonso, R. A. Baragiola, and A. Oliva-Florio, Surf. Sci. **120**, 427 (1982).
[8] D. E. Grosjean and R. A. Baragiola, in *Ionization of Solids by Heavy Particles*, edited by R. A. Baragiola (Plenum, New York 1992), p. 381.
[9] H. Jacobson and G. Holmén, Phys. Rev. B **49**, 1789 (1994).
[10] M. Vana, F. Aumayr, P. Varga, and H P. Winter, Nucl. Instrum. Methods Phys. Res. B **100**, 284 (1995).
[11] M. Shi, D. E. Grosjean, J. Schou, and R. A. Baragiola, Nucl. Instrum. Methods Phys. Res. B **96**, 524 (1995).
[12] J. Schou, Scanning Microsc. **2**, 607 (1988).
[13] R. E. Johnson, in *Ionization of Solids by Heavy Particles*, edited by R. A. Baragiola (Plenum, New York 1992), p. 419.
[14] G. Schiwietz *et al.*, Phys. Rev. Lett. **69**, 628 (1992).
[15] E. M. Gullikson and B. L. Henke, Phys. Rev. B **39**, 1 (1989).
[16] N. Schwentner *et al.*, Phys. Rev. Lett. **34**, 528 (1975).
[17] N. Schwentner, Phys. Rev. B **4**, 5490 (1976).
[18] P. Sigmund and S. Tougaard, in *Inelastic Particle-surface Collisions*, edited by E. Taglauer and W. Heiland (Springer-Verlag, Berlin, 1981), p. 2.
[19] W. O. Hofer, Scanning Microsc. Suppl. **4**, 265 (1990).
[20] M. Rösler, W. Brauer, J. Devooght, J.-C. Dehaes, A. Dubus, M. Cailler, and J.-P. Ganachaud, *Particle Induced Electron Emission I* (Springer-Verlag, Berlin, 1991).
[21] J. Schou, in *Ionization of Solids by Heavy Particles*, edited by R. Baragiola (Plenum, New York, 1993), p. 351.
[22] R. A. Baragiola, Nucl. Instrum. Methods Phys. Res. B **78**, 223 (1993).
[23] R. A. Baragiola, in *Low Energy Ion-Surface Interactions*, edited by J. W. Rabalais (Wiley, New York, 1994), Chap. 4.
[24] E. Gullikson, Phys. Rev. B **37**, 7904 (1988).
[25] E. M. Gullikson and A. P. Mills, Jr., Phys. Rev. B **39**, 6121 (1989).
[26] N. Sack and R. A. Baragiola, Phys. Rev. B **48**, 9973 (1993).
[27] D. E. Grosjean, Ph.D. thesis, University of Virginia, 1995.
[28] G. L. Pollack, Rev. Mod. Phys. **36**, 749 (1964).
[29] E. E. Koch, B. Raz, V. Saile, N. Schwentner, M. Skibowski, and W. Steinmann, Jpn. J. Appl. Phys., Suppl. **2**, 775 (1974).
[30] B. Sonntag, in *Rare Gas Solids*, edited by M. L. Klein and J. A. Venables (Academic, New York, 1977), Vol II, Chap. 17.
[31] D. E. Grosjean, R. A. Baragiola, and W. L. Brown, Phys. Rev. Lett. **74**, 1474 (1995).
[32] D. M. Schrader, A. Loewenschuss, J. Y. Jean, K. Nakamoto, and B. D. Pollard, in *Positron Annihilation*, edited by P. G. Coleman, S. C. Sharma, and L. M. Diana (North-Holland, Amsterdam, 1982), p. 657.
[33] Grain size increases with growth rate. See G. L. Pollack, Rev. Mod. Phys. **36**, 749 (1964).
[34] Trapped electrons produced by ionizing radiation can be released from the traps by increasing the temperature of the solid and recombine with trapped holes producing thermoluminescence. See A. N. Ogurtsov *et al.*, Low Temp. Phys. **22**, 922 (1996).
[35] A. Mozunder, Adv. Radia. Chem. **1**, 1 (1969).
[36] D. Srdoc, M. Inokuti, and I. Krajcar-Bronic, in *Atomic and Molecular Data for Radiotherapy and Radiation Research*, IAEA-TECDOC-799 (International Atomic Energy Agency, Vienna, 1995), Chap. 8.
[37] E. J. Sternglass, Phys. Rev. **108**, 1 (1957).
[38] J. Ferrón, E. Alonso, R. A. Baragiola, and A. Oliva Florio, Phys. Rev. B **24**, 4412 (1981).
[39] G. Schiwietz *et al.*, Phys. Rev. Lett. **61**, 2677 (1988).
[40] S. M. Ritzau and R. A. Baragiola, Phys. Rev. B **58**, 2529 (1998).
[41] J. F. Ziegler, *TRIM-96* (IBM, Yorktown Heights, 1996).
[42] H. H. Andersen and J. F. Ziegler, *Hydrogen Stopping Powers and Ranges in All Elements* (Pergamon, New York, 1977).
[43] R. A. Vidal, R. A. Baragiola, and J. Ferrón, J. Appl. Phys. **80**, 5653 (1996).
[44] N. Schwentner, E. E. Koch, and J. Jortner, *Electron Excitations in Condensed Rare Gases*, Springer Tracts in Modern Physics, Vol 107 (Springer, Berlin, 1985).
[45] E. Gullikson, Phys. Rev. B **37**, 7904 (1988).
[46] L. S. Miller, S. Howe, and W. E. Spear, Phys. Rev. **166**, 112 (1968).
[47] R. T. Scalettar, P. J. Doe, H.-J. Mahler, and H. H. Chen, Phys. Rev. A **25**, 2419 (1982).
[48] Simion 6.0 3D electrostatic analysis program, Idaho National Eng. Lab. Idaho Falls, ID.
[49] J. E. Marcoux, Can. J. Phys. **48**, 244 (1970).
[50] R. Gomer, *Field Emission and Field Ionization* (American Institute of Physics, New York, 1993).